Modeling of the calcium dynamics in Saccaromyces Cerevisiae for the International Genetically Engineered Machine competition

P.J. Alkema – 0658397
Bachelor Thesis

August 27, 2012

Supervisors:
Prof.dr. P.A.J. Hilbers
Eindhoven University of Technology
Department of Biomedical Engineering

Dr.ir. T.F.A. de Greef
Eindhoven University of Technology
Department of Biomedical Engineering

Abstract

A team of students from different departments of the Eindhoven University of Technology participate in the International Genetically Engineered Machine (iGEM) competition 2012, a synthetic biology competition for undergraduate students. The aim of the project of the team is to design and produce a multi-colored display, in which genetically engineered yeast cells are electrically controlled to induce a fluorescent light response. The main substance in this process is calcium. To investigate the dynamics of the calcium within a cell, a basic calcium model of yeast cells is formulated. This model is extended with overexpression of voltage-dependent calcium channels and addition of GECO-kinetics. The model will be used, together with experimental data, to justify the results of the iGEM team of the Eindhoven University of Technology in 2012.

Contents

Chapter 1

Introduction

1.1 Synthetic Biology

The drive to develop 'a technology of the living substance' has fascinated scientists for centuries and has led to several moments in history when scientists claimed they were about to 'create life in the test tube', produce 'synthetic new species' at will, or otherwise engage in the engineering of genes and chromosomes. Synthetic biology aims to build artificial biological systems for engineering applications, using many of the same tools and experimental techniques [1]. The title 'synthetic biology' appeared in the literature in 1980, when it was used by Barbara Hobom to describe bacteria that had been genetically engineered using recombinant DNA technology [2]. The focus is often on ways of taking parts of natural biological systems, characterizing and simplifying them, and using them as a component of a highly unnatural, engineered, biological system [1]. The individual parts are standardized by engineers, e.g. DNA BioBricks^{TM}. The BioBricks^{TM} are collected in the Registry of Standard Biological Parts, a continuously growing collection of genetic parts, founded in 2003 at Massachusetts Institute of Technology.

Synthetic biology already has many accomplishments to its credit. The effort to generate synthetic genetic systems has yielded diagnostic tools, such as Bayer's branched DNA assay, which annually helps to improve the care of some 400.000 patients infected with HIV and hepatitis viruses. Also synthetic biology has generated some interesting toys from biomolecular parts, including systems that oscillate and that carry out simple computations. As an introduction to synthetic biology, two early research projects will be discussed.

1.1.1 A Synthetic Oscillatory Network

One of the first articles on synthetic biology describes the design and construction of a synthetic network to implement a particular function. A three transcriptional repressor system was used to build an oscillating network, termed the repressilator, in Escherichia Coli. As a readout of the network states in individual cells, the synthesis of a green fluorescent protein was induced periodically.

In order to describe the behavior of the system the concentrations of the three repressor-protein concentrations and their corresponding mRNA concentrations were treated as continuous dynamical variables. Six coupled first-order differential equations can be derived by making use of the Hill equations. The period of oscillations in such networks is determined mainly by the protein stability. Since the interaction between the molecular components has a stochastic character, an discrete approximation was also published. Therefore the presence of two operator sites on each promotor were assumed and the parameters were chosen to correspond as closely as possible to the continuous model described before [3].

1.1.2 Bistable Switch

Bistable systems have memory. That is, when switched to one state or another, these systems remain in that state unless forced to change back. The light switch is a common example of a bistable system from everyday life. The genetic toggle switch consists of two genes, each of which encodes for a protein that represses the other's gene expression. Because of the even number of components in the circuit, there is a net positive feedback, which can give rise to bistable behavior for certain parameter values.

Equations 1.1 and 1.2 form the dimensionless model for the network, which presents the behavior of the toggle switch and the states of bistability:

$$\frac{du}{dt} = \frac{\alpha_1}{1 + v^\beta} - u \tag{1.1}$$

$$\frac{dv}{dt} = \frac{\alpha_2}{1 + u^\gamma} - v \tag{1.2}$$

In these equations, u is the concentration of Repressor 1, v is the concentration of Repressor 2, α_1 is the effective rate of the synthesis of Repressor 1, α_2 is the effective rate of the synthesis of Repressor 2, β is the cooperativity of the repression of Promoter 2 and γ is the cooperativity of the repression of Promoter 1.

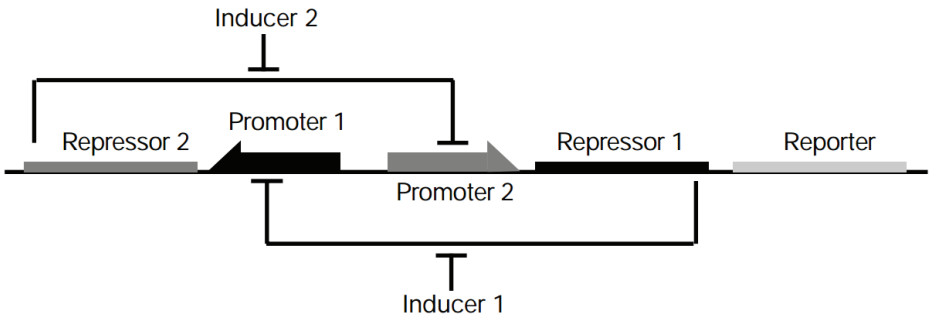

Figure 1.1: Toggle switch design. Repressor 1 inhibits transcription from Promoter 1 and is induced by Inducer 1. Repressor 2 inhibits transcription from Promoter 2 and is induced by Inducer 2 [4].

A biochemical rate equation formulation of gene expression forms the basic principle of this model. In each equation, the first term represents the cooperative repression of the continuous transcribed promoters and the second term represents the degradation or dilution of the

repressors. For the toggle switch equations, these are the two most fundamental aspects of the network.

1.2 iGEM

The International Genetically Engineered Machine competition (iGEM) is the premiere undergraduate synthetic biology competition and started in January 2003. Student teams are given a kit of biological parts from the Registry of Standard Biological Parts, as mentioned before. During the research they will make use of the known BioBricks^{TM} and develop new BioBricks^{TM} that will be added to the registry. The organization promotes the advancement of science and education by developing an open community of students and practitioners in schools, laboratories, research institutes and industry.

The research described in this thesis is part of the research done by the iGEM team of the Eindhoven University of Technology in 2012 and will be presented during the European iGEM Jamboree, 5-7 October 2012.

1.3 Project Selection

In order to make a chance to reach the iGEM competition finals, a dashing project has to be chosen. To be inventive, it is important to know what is renewing within the field of synthetic biology and within the iGEM competition. For this purpose, all projects of previous years are regarded and the most remarkable projects are discussed during several group meetings. Furthermore, all new and interesting articles of the 'Science' and 'Nature' journals have been read. To stimulate the creativity within the group, a brainstorm session was held. The group members came up with a great variety of topics, from bacterial anti-aging cream to oil detecting bacteria and from bio batteries to anti-hangover medicines. Of all these subjects, the most interesting and most significant topics were chosen to be elaborated. After extensive research and decision making, four topics remained.

1.3.1 Bacterial CSI

At a crime scene, the victim as well as the offender leaves traces. When these traces are investigated, the delinquent can easily be found and judged. For blood samples, finger prints and gunshot residues, proper materials are available. To wage war against crime, the iGEM team of the Eindhoven University of Technology in 2012 thought of a way to collect DNA at a crime scene. Scientists have tried to transform several kinds of bacteria in order to introduce exogenous DNA to the cell. Usually this is done by altering the permeability of the cell membrane. However, bacteria which are naturally able to take up DNA from the extracellular environment do exist [5]. Protein complexes help to transport one strand of the incoming DNA through the cell wall and cell membranes, while the second strand will be degraded and released into the extracellular milieu. The uptake of DNA can be sequence specific. This might help to take up only human DNA. After the uptake, protein transcription

will be activated. With the use of a fluorescent label, bacteria can show whether they have taken up exogenous DNA.

1.3.2 Facebook

Nowadays, 'Facebook' is one of the most important social media services available on the internet. Based on the principle of social networking, the iGEM team wanted to reduce these networks to nano-scale. The bacteria-based nanonetwork should be made on a liquid medium and consists of so called nodes and carriers [6]. The nodes try to communicate with each other by exchanging messages. The messages will be encoded in a plasmid, circular double-stranded DNA. The carriers will take up the DNA and swim through the liquid medium to another node, using flagella. Flagella are tail-like extensions which the bacteria use to move. Each node emits its own chemical attractant. Due to this, the sending nodes can address a specific receiver node. The carriers move to the chemical attractants by the use of chemotaxis. Chemotaxis is the movement of bacteria into a certain direction due to chemical concentration gradients. When the carriers are arrived at the right node, the plasmid will be transferred to this node and the message will be decoded.

The handouts of the presentation of this project proposal can be found in appendix **??**.

1.3.3 Tumortargeting

Cancer is one of the most occurring lethal diseases. Many scientists are looking for 'the cure for cancer', but it has not been found yet. By this project, the iGEM team wanted to become a part of this research group, to make a difference in the world. Tumor cells are active cells and therefore spread lactic acids [7]. Using chemotaxis, bacteria can move to acid environments to reach the tumor cells. After binding to the tumor cells, the bacteria will disperse signaling molecules. With the use of the quorum sensing mechanism, more signaling molecules will be spread. Quorum sensing is a positive regulating mechanism controlled by population density. The more bacteria are present, the more signaling molecules are dispersed, the more new signaling molecules are made and dispersed. To gather the bacteria, swarming motility, the movement of bacteria due to signaling molecules, will be used. After gathering the bacteria, the tumor cells will be destroyed.

1.3.4 TV Screen

Sensational things can be done with light. An example is 'GLOW', the international forum of light in art and architecture in Eindhoven. To promote Eindhoven as 'the city of light', the iGEM team came up with the idea to make a TV screen of yeast. The basis of the TV screen will be a foil with electrodes on which the yeast will be spread. The electrodes will be controlled by software like LabVIEW. The yeast will contain three different voltage-gated calcium channels. When an electrical current is set onto the calcium channel, the calcium will be transported in the cell [7]. In the cell, the calcium will bind to a green fluorescent protein [8]. After connection, the green fluorescent protein will be activated and will send out fluorescent light. Green fluorescent proteins are available in different colors. To imitate

an actual TV, the colors green, blue and red will be used in combination with the different voltage-gated calcium channels. When the calcium is released, the fluorescent light will go off.

These topics were presented to the supervisors. The possibilities and limitations of the knowledge and technical and biological requirements of the Eindhoven University of Technology were considered and consulted. 'Bacterial CSI', 'Facebook' and 'Tumortargeting' were rejected, because of many uncertainties, ethical problems and the lack of guarantees for results. The topic 'TV screen' seemed the perfect project and is therefore elected as the project for the iGEM 2012 competition.

Chapter 2

Project Overview

Although this thesis covers the research of the calcium model, a small introduction to the total project is given.

2.1 Light Emitting Cells

A 'Light Emitting Cell' (LEC) is a living cell that responds to electric signals by emitting light. Previous research has shown the possibility of creating displays using LECs, albeit with strict limits on resolution and refresh rate.

A display converts electric signals into spatially distributed light. A commonly used architecture is an orthogonal grid (matrix) of light emitting picture elements (pixels). Each pixel is controlled by an electrode that dictates the desired emission intensity. The most basic form is a monochrome display in which pixels are either on or off. Luminescence of the pixels can be achieved in many ways physically, for example through Light Emitting Diodes (LED) in LED displays or back lighting in a Liquid Crystal Display (LCD). The time required to change from one clearly visible image to the next is called the refresh rate (Hz).

2.2 iGEM Team Valencia 2009

In 2009 the iGEM team of Valencia presented the 'iGEM Valencia's Lightning Cell Display', the new iLCD: a 'bio-screen' of voltage activated cells, where every 'cellular pixel' produces light. This research on light emitting cells as a response to electrical stimulations can be seen as the basis of the project of the iGEM team of the Eindhoven University of Technology in 2012.

One of the main goals of the iGEM competition is making use of other teams and their projects. The team used a genetically modified yeast strain expressing the protein aequorin. Upon the release of calcium into the cytosol through voltage-dependent calcium channels, luminescence of aequorin shortly increased a thousand-fold compared to the steady state luminescence. These cells were cultured in medium on a 96-wells plate with a separate

electrode inserted into each well to supply a transient electric pulse to depolarize the cell membrane and cause calcium influx into the cytosol, leading to luminescence of aequorin. The obtained refresh rates were in the order of 0.1 Hz.

2.3 Project Plan

In Saccaromyces cerevisiae, known as budding yeast, voltage-dependent calcium channels are present in the plasma membrane. These calcium channels are made of CCH1 and MID1 proteins. Depolarization of the plasma membrane will open these channels and cause a calcium ion influx. The voltage-dependent channels may be overproduced, using co-overexpression of the CCH1 and MID1 genes from high-copy number plasmids, to increase the calcium influx upon electrical stimulation [9]. At high electric fields, the cells may be lysed by electrical stimulation. In order to find the safe range for electrical stimulation which can be used in the final display, test cells will be exposed to increasing field strengths until lysis occurs.

Recent work reported several calcium dependent fluorescent proteins that can be used as a calcium modulated light source [10]. At low concentrations, relative to homeostatic levels, the protein is not fluorescent, while at high concentrations, relative to levels directly after influx, the protein is fluorescent. Moreover, variants emitting different colors of light have been developed. Three variants are of particular interest for this project: B-GECO1 (blue), R-GECO1 (red) and G-GECO1.1 (green). The DNA sequences of these variants are available on www.addgene.org, a non-profit plasmid sharing service. The encoding gene from the plasmid will be inserted into a suitable expression vector. The yeast cells are then transformed with the vector.

Directly after the influx of the calcium ions into the cytosol, the calcium concentration will be above the homeostatic value and GECO proteins in the cytosol will start to fluoresce. After a certain period the concentration will decrease by active transport. This will stop the fluorescence of the GECO proteins. In this way, a genetically engineered electrical stimulated LEC is made. In chapter 3 the kinetics of the GECO proteins are discussed in more detail.

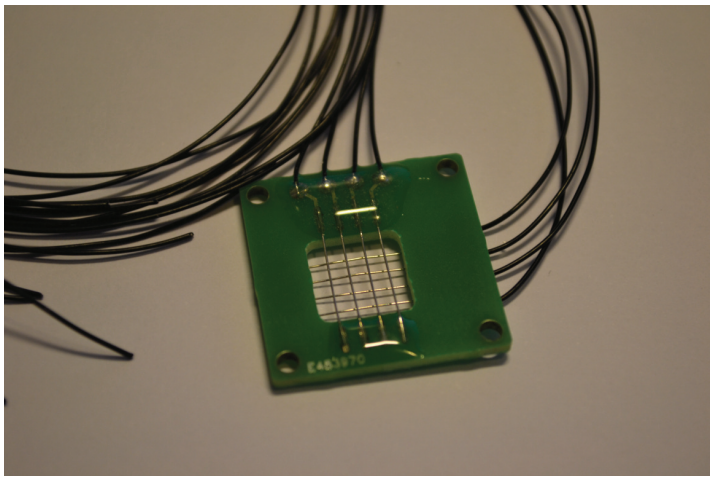

Figure 2.1: The device: the electrodes without the growth medium

Because living cells require a suitable substrate and growth medium, the display design requires an alternative matrix architecture to control the pixels. The electrical input will be given by a separate device connected to the display. The device is displayed in figure 2.1. Since the cells are fluorescent, they do not produce light themselves. The device should contain a lamp and should be as transparant as possible, because light needs to pass through the bottom as wel as the top. Furthermore, the device may not react with the growth medium in any way.

2.4 Goal

The aim of this project of the iGEM team of the Eindhoven University of Technology in 2012 is to design and produce a new multi-colored display in which genetically engineered cells are electrically controlled to induce a fluorescent light response. The largest challenge can be found in increasing the refresh rate of the screen. Therefore a model of the calcium concentration inside the cell is required to examine the influence of the different parameters on the decrease of the calcium concentration. Analysis of this dynamic model may yield critical design parameters that can be altered experimentally to increase the refresh rate.

Chapter 3

Calcium Model

Biological cells use highly regulated homeostasis systems to keep a very low cytosolic Ca^{2+} level. In normal-growing yeast the cytosolic Ca^{2+} concentration is maintained in the range of $50 - 200nM$ in the presence of environmental Ca^{2+} concentrations ranging from $< 1\mu M$ to $> 100mM$ [11]. To achieve an accurate model, the influences of voltage-dependent calcium channels are added to a basic model for yeast calcium homeostasis. In this model, first described by J. Cui *et al*, the main contributions of calcium transport are defined [12].

In literature, little can be found about modeling calcium channels in Saccaromyces Cerevisiae, most commonly known as budding yeast. Our model of calcium channels in yeast is based on a basic model of sympathetic ganglion 'B' type cells of a bullfrog [19] is used. This is a type of nerve cells that exists in nerve junctions of the orthosympathetic nervous system. At first the complete model of the bullfrog cells was used by C. Balemans, team member of iGEM team of the Eindhoven University of Technology in 2012, to describe the cytosolic Ca^{2+} level in yeast cells [13]. In this research the model is more focused on protein modeling, including the GECO proteins.

The model is made in MATLAB and the code can be found in appendix **??**.

3.1 Calcium homeostatic process in yeast cells

The homeostatis system in yeast cells, as mentioned before, has two basic characteristics. The cytosolic Ca^{2+} concentration is tightly controlled by "zero" steady-state error to extracellular stimuli and the system is relatively insensitive to specific kinetic parameters, due to robustness of such adaptation [14]. This second characteristic will be discussed in more detail in chapter 4.

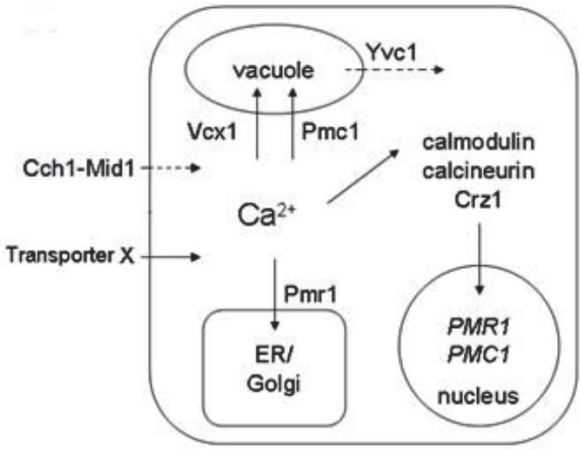

Figure 3.1: A schematic graph illustrating the protein level observations of the yeast calcium homeostasis system. Channel Cch1-Mid1 on the plasma membrane opens only under abnormal conditions. The vacuole can release Ca^{2+} into the cytosol through Yvc1, though only under the abnormal conditions of an extracellular hypertonic shock [12].

Under normal conditions, extracellular Ca^{2+} enters the cytosol through an unknown Transporter X, whose encoded gene has not been identified yet. Cytosolic Ca^{2+} can be pumped into endoplasmic reticulum (ER) and Golgi system through Pmr1 and can be sequestered into the vacuole through Pmc1 and Vcx1. Both the expression and function of Pmc1, Pmr1 and Vcx1 are regulated by calcineurin, a highly conserved protein phosphatase that is activated by Ca^{2+}-bound calmodulin [12].

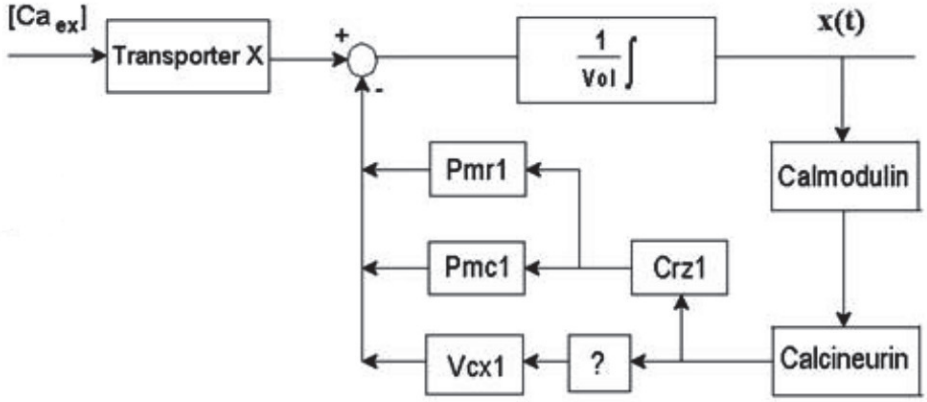

Figure 3.2: Block diagram of calcium homeostasis under normal conditions. Through unknown Transporter X, extracellular Ca^{2+}, denoted by $[Ca_{ex}]$, enters the cell. Proteins Pmr1, Pmc1 and Vcx1 cause feedback control through calmodulin and calcineurin. Crz1 is a transciptional factor and '?' denotes an unknown mechanism [12].

3.2 Feedback modeling

3.2.1 Sensing cytosolic Ca^{2+}

Calmodulin is a Ca^{2+}-binding protein expressed in all eukaryotic cells. The protein binds to cytosolic Ca^{2+} as a response to an increase of the Ca^{2+} level in the cell. A host domain for target proteins, including calcineurin, is activated. In yeast cells, calmodulin can only bind to a maximum of three molecules of Ca^{2+} [15]. A strong cooperativity among the three active sites can be assumed. Therefore the cytosolic Ca^{2+} sensing process can be described as follows:

$$3Ca^{2+} + Calmodulin \rightleftharpoons CaM \tag{3.1}$$

where CaM denotes Ca^{2+}-bound calmodulin. The concentration of Ca^{2+}-bound calmodulin will be denoted as CaM(t) and can be described by mass-action kinetics with forward rate constant k_M^+ and backward rate constant k_M^- as follows:

$$\frac{dCaM(t)}{dt} = k_M^+([CaM_{total}] - CaM(t)) \cdot Ca(t)^3 - k_M^- CaM(t) \tag{3.2}$$

where $[CaM_{total}]$ denotes the total concentration of calmodulin, the sum of Ca^{2+}-free and Ca^{2+}-bound calmodulin.

3.2.2 Calcineurin activation

Upon elevation of cytosolic Ca^{2+}, Ca^{2+}-bound calmodulin binds to the catalytic subunit of calcineurin and activates calcineurin by displacing the carboxyl-terminal autoinhibitory domain. This binding process can be described as:

$$CaM + Calcineurin \rightleftharpoons CaN \tag{3.3}$$

where CaN denotes activated calcineurin. The concentration of Ca^{2+}-bound calneurin will be denoted as CaN(t) and can be described by mass-action kinetics with forward rate constant k_N^+ and backward rate constant k_N^-. Since each molecule of calcineurin binds with one molecule of Ca^{2+}-bound calmodulin, we can derive the following equation:

$$\frac{dCaN(t)}{dt} = k_N^+([CaN_{total}] - CaN(t)) \cdot CaM(t) - k_M^- CaN(t) \tag{3.4}$$

where $[CaN_{total}]$ denotes the total concentration of calcineurin, the sum of Ca^{2+}-free and Ca^{2+}-bound calcineurin.

3.2.3 Gene expression control

Experimental results show that activated calcineurin regulates the production of the proteins Pmc1 and Pmr1 by controlling the synthesis of these two proteins through a transcription

factor Crz1 [16]. Crz1 is a highly phosphorylated protein that can be dephosporylated by activated calcineurin. We assume that only fully dephosphorylated Crz1 molecules in the nucleus are transcriptionally active since this has been shown the case for NFAT1. The mechanism of Crz1 translocation in yeast cells is similar to NFAT (nuclear factor of activated T-cells) translocation in mammalian T-cells. Therefore, some of the parameters stated in this chapter are based on experimental data on NFAT1. A conformational switch model is used to simulate Crz1 translocation, as described by Okamura *et al* [17]. By describing the conformational switch model as a protein network and using the rapid equilibrium approximation [18], we can use the following equation to describe the kinetics of the total nuclear Crz1 fraction which is denoted by Crz(t):

$$\frac{dCrz(t)}{dt} = d \cdot \phi(1/CaN(t)) \cdot (1 - Crz(t)) - f \cdot (1 - \phi(1/CaN(t))) \cdot Crz(t) \tag{3.5}$$

d denotes the import rate constant, f denotes the export rate constant and ϕ denotes the ratio of the fraction of the cytosolic active conformation over the total cytosolic fraction:

$$\phi(y) = 1/(1 + L_0 \cdot \frac{(\lambda y)^{N+1} - 1}{\lambda y - 1} \cdot \frac{y - 1}{(y)^{N+1} - 1}) \tag{3.6}$$

where N is the number of relevant regulatory phosporylation sites, experimental data shows that $N = 13$ in the case of NFAT1. L_0 denotes the basic equilibrium constant and λ is the increment factor. The conformational switch model and deduction of the function $\frac{dCrz(t)}{dt}$ is described in more detail in appendix C.

As mentioned before, Crz1 is a transcription factor which controls the synthesis of Pmc1 and Pmr1. The concentrations of these two proteins are assumed to be proportional to transcriptionally active Crz1 fraction in the nucleus and therefore:

$$[Pmc1] = k_a \cdot h(t) \cdot \theta(1/z(t)) \tag{3.7}$$

$$[Pmc1] = k_b \cdot h(t) \cdot \theta(1/z(t)) \tag{3.8}$$

where $[Pmc1]$ and $[Pmr1]$ denote the concentrations Pmc1 and Pmr1 respectively and k_a, k_b denote the feedback control constants.

For the feedback regulation of activated calcineurin on the synthesis of Vcx1, the process is stil unknown. The only knowledge about this regulation is that the mechanism is possibly posttranslational and the general effect is suppressing. As an approximation this regulation is expressed as follows [12]:

$$[Vcx1] = k_d/(1 + k_c \cdot CaN(t)) \tag{3.9}$$

where k_c and k_d denote the feedback control constants. As stated by this equation, the concentration of Vcx1 will drop when CaN(t) rises.

3.3 Protein modeling

All four involved proteins (Transporter X, Pmc1, Pmr1 and Vcx1) can be described by the Michaelis-Menten kinetics, often used to describe simple enzymatic reactions. For example, the uptake rate of Transporter X, k, can be described by:

$$k = \frac{V_{max} \cdot [Ca_{ex}]}{K_x + [Ca_{ex}]} \tag{3.10}$$

where $V_{max}(\mu M s^{-1})$ is the maximum uptake rate of Transporter X and $K_x(\mu M)$ is the binding constant.

3.3.1 GECO proteins

The iGEM team of the Eindhoven University of Technology in 2012 uses the fluorescent activity of CMV-X-GECO.1 proteins as light-emitting part of the cell, as a result of an increase of the cytosolic Ca^{2+}-level. Therefore, also the kinetics of calcium binding by these G-GECO proteins need to be taken into account. Although three different GECO proteins are used (CMV-R-GECO1, CMV-G-GECO1.1 and CMV-B-GECO1) to provide different colors, only the variant CMV-G-GECO1.1 is discussed. The kinectic characterization of the different GECOs can be found in table 3.1. Upon elevation of cytosolic Ca^{2+}-level, Ca^{2+} binds to the GECO protein, a process that we can described as follow:

$$nCa^{2+} + GECO \rightleftharpoons CaGECO \tag{3.11}$$

where $CaGECO$ denotes Ca^{2+}-bound GECO protein and n the number of Ca^{2+} molecules that binds to the protein. This equation yields a forward rate constant k_{on} and a backward rate constant k_{off} as mentioned in table 3.1.

Protein	$k_{on}(M^{-n}s^{-1})$	$k_{off}(s^{-}1)$	n	$K_{d,kinetic}(nM)$	$K_{d,static}(nM)$
R-GECO1	$9.52 \cdot 10^{9}$	0.752	1.6	484	482
G-GECO1.1	$8.17 \cdot 10^{15}$	0.675	2.6	809	618
B-GECO1	$4.68 \cdot 10^{12}$	0.490	2.0	324	164

Table 3.1: Kinetic characterization of GECO proteins [10].

We can assume $[GECO_{total}]$, the total concentration of GECO (including Ca^{2+}-bound and Ca^{2+}-free form) to be constant. If we further denote the concentration of Ca^{2+}-bound GECO protein as $CaGECO(t)$, then according to the law of mass action, we can derive the time dependence of $CaGECO(t)$ as follows:

$$CaGECO'(t) = k_{on}([GECO_{total}] - CaGECO(t)) \cdot Ca(t)^n - k_{off} CaGECO(t) \tag{3.12}$$

3.4 Ionic Current Flow

The largest flux of calcium ions into the cell occurs via voltage-dependent channels. Equation 3.13 [19] shows the change in calcium concentration in the cell on account of the influx, with $[Ca^{2+}]$ the intracellular calcium concentration (mM), $I_{Ca^{2+}}$ the calcium current (nA) and V_n the volume of the cell (l). Faraday's constant, F, converts the quantity of moles to the quantity of charge for a univalent ion [20].

$$\frac{\partial[Ca^{2+}]}{\partial t} = \frac{-I_{Ca^{2+}}}{2FV_n} \tag{3.13}$$

Generally, ionic currents can be described by Ohm's law [19]:

$$I(t) = g(t, V) \cdot (V - E) \tag{3.14}$$

In this equation, g is the time and voltage dependent conductance (μS), V is the voltage (mV) and E is the Nernst potential (mV). The conductance associated with the channel can be calculated by equation 3.15 [19], with $\bar{g}$ the maximum conductance of the membrane, m the activation variable $(-)$, h the inactivation variable $(-)$ and i and j positive integers.

$$g(t, V) = \bar{g} \cdot m(t, V)^i \cdot h(t, V)^j \tag{3.15}$$

The dynamics of the activation variable can be found using equation 3.16 [19], where m_∞ is the steady state value of m and τ_m is a characteristic time constant (s).

$$\frac{dm(t, V)}{dt} = \frac{m_\infty(V) - m(t, V)}{\tau_m(V)} \tag{3.16}$$

The steady state value of m, m_∞, and the time constant, τ_m, can be described using the Hodgkin-Huxley equations. Equations 3.17 [19] and 3.18 [19] are the Hodgkin-Huxley equation, suited for the calcium influx.

$$\tau_m = \frac{7.8}{e^{+(V+6)/16} + e^{-(V+6)/16}} \tag{3.17}$$

$$m_\infty = \frac{1}{1 + e^{-(V-3)/8}} \tag{3.18}$$

The dynamics of the inactivation variable is given by equation 3.19 [19], a simple Michaelis-Menten equation, with K an equilibrium constant related to the concentration at which inactivation is halfway (μM).

$$h_{Ca^{2+}} = \frac{K}{K + [Ca^{2+}]} \tag{3.19}$$

Equation 3.20 [19] is the Nernst equation for calcium.

$$E_{Ca^{2+}} = 12.5 log \frac{[Ca^{2+}]_{ex}}{[Ca^{2+}]} \tag{3.20}$$

In this equation, $[Ca^{2+}]_{ex}$ is the constant extracellular calcium concentration (μM).

3.5 Cytosolic calcium level

As a result of the uptake models for all the involved proteins, including the GECO proteins, models for the relevant feedback regulation and models for the calcium channels, the main equation for the concentration of cytosolic calcium can be derived:

$$\begin{aligned}\frac{dCa(t)}{dt} = & \underbrace{\frac{V_x \cdot [Ca_{ex}]}{K_x + [Ca_{ex}]}}_{TransporterX} - \underbrace{Crz(t)\theta(\frac{1}{CaN(t)})\frac{V_1 \cdot Ca(t)}{K_1 + Ca(t)}}_{Pmc1} \\ & - \underbrace{Crz(t)\theta(\frac{1}{CaN(t)})\frac{V_2 \cdot Ca(t)}{K_2 + Ca(t)}}_{Pmr1} - \underbrace{\frac{1}{1 + k_c CaN(t)}\frac{V_3 \cdot Ca(t)}{K_3 + Ca(t)}}_{Vcx1} \\ & - \underbrace{n(k_{on} \cdot CaGECO(t) - k_{off} \cdot Ca(t)^n([CaGECO_{total}] - CaGECO(t)))}_{GECO} \\ & - \alpha Ca(t) \end{aligned} \tag{3.21}$$

The final model consists of six equations (Eqs. 3.4, 3.2, 3.12, 3.5, 3.21, 3.16) and six unknowns: $CaN(t)$, $CaM(t)$, $CaGECO(t)$, $Crz(t)$, $Ca(t)$ and $m(t)$.

3.6 Calcium Diffusion

After entering the cell, the calcium will be transported through the cell by diffusion. Since the cell is sphere-like, the diffusion equation will be formulated in spherical coordinates. When the tangential components are neglected, the three-dimensional equation is reduced to a one-dimensional problem, which can be found in equation 3.22 [19].

$$\frac{\partial r[Ca^{2+}]}{\partial t} = D\frac{\partial^2 r[Ca^{2+}]}{\partial r^2} \tag{3.22}$$

In this equation, D is the diffusion constant ($\mu m^2 s^{-1}$) and r is the radius of the cell (μm). Because of the dependence on both space and time and the complexity to model this, the calcium diffusion in the cell is neglected in our first attempt to model calcium dynamics in the cell. However, in order to reliably predict calcium dynamics in the cell, future studies should address the role of diffusion.

Chapter 4

Analysis

An analysis of the used parameters and the results is performed for the dynamic calcium model as described in the previous chapter. The model consists of six equations (Eqs. 3.2, 3.4, 3.12, 3.5, 3.21, 3.16) and six unknowns: $CaM(t)$, $CaN(t)$, $CaGECO(t)$, $Crz(t)$, $Ca(t)$ and $m(t)$.

4.1 Parameter Values

To simulate the model, realistic parameter values should be implemented. The parameters described by J. Cui *et al* in their model for yeast calcium homeostasis are well thought-out and mostly justified by different sources. Since the model of the voltage-dependent calcium channels is a model of sympathetic ganglion 'B' type cells of a bullfrog as described in '*Methods in Neuronal Modeling: From Synapses to Networks*' [19], all relevant parameter values are taken from this book of reference. In order to fit into the basic model, the units of these parameters were adjusted. In table 4.1, the initial values are shown. In appendix F the model parameters for which all results are calculated, unless otherwise stated, are shown.

To see the effect on the calcium concentration when a voltage is supplied to the cell, a pulse is applied as the input of the dynamic model, as shown in table 4.2.

The calculations are done for a time span of $20s$. The results are shown in appendices B and C, the described symbols are listed in appendix A.

Parameter	Initial value
$[CaM]$	0 μM
$[CaN]$	0 μM
$[CaGECO]$	0 μM
$[Crz]$	0 μM
$[Ca^{2+}]$	10 μM
m	0.41

Table 4.1: Initial values

Variable	Value	Used assumption
V	-50 mV	The resting potential of this type of yeast cell, due to the difference of the mix of positive and negative charged ions in the cell and in the extracellular environment
V	32 mV	Every other three seconds the cell is supplied with a voltage of $V = 32$ mV with a duration of $1s$

Table 4.2: Voltage values

4.2 Results

As we could not yet accomplish a complete sensitivity analysis on the model, we only consider the basic characteristics of the different parts of the model. Furthermore, the influences of some basic experimental setup values are stated, i.e. the concentration of extracellular calcium, $[Ca]_{ex}$, and the duration of the pulse. The figures mentioned in this section can be found in appendices B and C.

As shown in figure B.1, the basic model for calcium homeostasis in yeast cells shows an oscillatory system. As a result of the increase of the cytosolic Ca^{2+}-level, the concentrations $[CaM]$ and $[CaN]$ also increase, since calmodulin and calcineurin bind to calcium. Due to the negative feedback system caused by the protein Vcx1, the cytosolic Ca^{2+}-level decreases after obtaining a maximum value. This maximum value seems to be constant in time. In figure B.2, a different initial value of the cytosolic Ca^{2+} level is used, $20\mu M$ instead of $10\mu M$ in figure B.1. This initial value does not seem to influence the overall values of the final state.

The concentration of $[Ca^{2+}]_{ex}$, however, does influence the behavior of the oscillation. In table 4.3 the different times for one period of oscillation are shown. Looking at these values, it is shown that the decrease of this parameter has approximately the an increasing effect on the oscillation time of the system.

$[Ca^{2+}]_{ex}$	Oscillatory period
10 μM	2 seconds
25 μM	2.5 seconds
50 μM	3.3 seconds

Table 4.3: Oscillatory period for different values of $[Ca^{2+}]_{ex}$

Furthermore, we need to look into the results of the complete model, including the kinetics of the GECO-proteins and the characteristics of the voltage-dependent calcium channels. In figures C.1 and C.2 multiple pulses are shown, with different duration times. During the pulse, the calcium concentration increases and therefore also the concentrations of CaGECO and CaM. On the other hand, $[Crz]$ turns out to be constant in time and therefore no oscillatory system can be observed. After the pulse, the calcium concentration decreases remarkably fast, while the concentration of the GECO-calcium complex decreases much slower, as expected.

Looking at the results of the model in more detail, fig. C.3, with a pulse duration of one second, the different influences of the specific parts of the model can be made more clear. Since the calcium level increases as a response to the pulse, both calmodulin and the GECO-protein

will bind to calcium. Therefore, both $[CaM]$ and $[CaGECO]$ will reach their maximum. Next to it, the graphs of $[CaN]$ show clear influences of $[CaM]$. This is caused by the fact that calcineurin binds to calcium-bounded calmodulin.

When a shorter opening time of the calcium channels is modeled, fig C.3, almost the same Ca^{2+}-level is reached. When the opening time of the calcium channels is reduced even more (fig. C.4, C.5), the $[Ca^{2+}]$-level does not reach the same maximum anymore. Both calmodulin and the GECO-protein are in total bounded to $[Ca^{2+}]$. Since this is only for a short duration, $[CaN]$ does not reach same level as for larger opening times. The figures C.3, C.4 and C.5 however have a similar shape when it comes to the decrease of $[CaGECO]$, since the same maximum of $[CaGECO]$ is reached.

4.3 Discussion

One of the most important points of discussion is the overall correctness of the calcium model. Due to the fact that the characteristics of both the voltage-dependent calcium channels and the GECO-proteins are added to the calcium homeostasis of the organism Saccaromyces Cerevisiae, a completely new system is created. As far as we know, in literature, no experimental data can be found about this specific system. At the moment of writing, the wetwork of the iGEM team of Eindhoven University of Technology 2012 is unfortunately not able to provide applicable information. A great step forward could be made when this model can be checked with experimental data. Nevertheless this model does give some quantitative insight in the behavior.

The simplification of the calcium homeostasis in a living yeast cell certainly leads to some imperfections upon the level of the actual physiology. For example, in the current model, we assume that the concentrations of Pmc1 and Pmr1 are directly proportional to the quantity of transcriptionally active Crz1. This is a big simplification since in real cells, this process involves the increased gene expression through Crz1 followed by translation and transport of the proteins to the respective intracellular destinations. Moreover, the current model does not include the influence from other relevant pathways whereas in real cells, any response to given extracellular stimulus is likely to be the result of complex cross-talk between multiple pathways.

Also some other assumptions need to be taken into account. First, we assumed that only fully dephosphorylated Crz1 molecules in the nucleus are transcriptionally active since this has been shown the case for NFAT1. Although the mechanism of Crz1 translocation in yeast cells is strikingly similar to NFAT, not all processes can be regarded the same, since there are no experimental data found to validate this assumption. Second, we assumed the behavior of the voltage-dependent calcium channels in yeast cells to be the same as in sympathetic ganglion 'B' type cells of a bullfrog.

The results, as presented in the previous section, show a large drop of the cytosolic Ca^{2+}-level after removal of the potential difference. Although we could expect a fast recovery to the steady state, this drop is remarkably fast. This is one of the unexpected results of this model and therefore one of the more interesting parts to check with the experimental data. Especially since this drop will influence the concentration of calcium bounded GECO-protein.

In order to provide more quantitative insights in the experimental setup for the total project, we have to obtain information about the fluorescent properties of the GECO-proteins. At this moment we can only predict when the CaGECO concentration reaches a set percentage of the maximum amount of Ca^{2+}-bounded GECO-protein. An important value is the amount of calcium bounded GECO-protein that needs to be there in order to detect fluorescent light.

Chapter 5

Conclusion and Outlook

The goal of the project of the iGEM team of Eindhoven University of Technology in 2012 is to design and produce a multi-colored display, in which genetically engineered cells are electrically controlled to induce a fluorescent light response. In this process, calcium is one of the most important substances. To examine the calcium in the cell, a dynamic calcium model was designed. As a start a basic model of calcium homeostasis in yeast cells was presented and tested. This model was extended with overexpression of voltage-dependent calcium channels and addition of GECO-kinetics. With this model, we can test and verify theoretical hypotheses by comparing simulation results with corresponding experimental results and generate new hypotheses on the regulation of calcium homeostasis. On the other hand, due to the existence of unknown factors and the lack of experimental data, this model is not an exact model yet. However, it does can give some quantitative insight into the possible dynamics of the whole process and provide a general framework for more elaborate investigations.

To improve the model for the aim of the project, the parameters in the model will be adapted, using of experimental data, to predict the calcium dynamics in yeast cells. A complete sensitivity analysis needs to be applied, in order to determine the best settings for the experiments, i.e. the concentration of the extracellular Ca^{2+} concentration.

Furthermore, the influence of calcium diffusion through the cell will be taken into account in an extended model. Instead of MATLAB, COMSOL simulation software will be used, because it is less complex to model dependency on both space and time in COMSOL. Subsequently, the results of the model will be compared to the results of the experiments. The response of the yeast cells to the electric stimulation will be improved by altering the genetic code utilizing existing BioBricks^{TM} and developing new ones, using the results of the model.

Appendix A

Symbols

Symbol	Value	Unit	Description
$[Ca^{2+}]$		micromolar (μM)	Cytosolic calcium concentration
$[Ca^{2+}_{ex}]$	1	micromolar (μM)	Constant extracellular calcium concentration
$[GECO_{total}]$	25	micromolar (μM)	the total concentration of Ca^{2+}-binded GECO
$[CaN_{total}]$	25	$(-)$	the total concentration of calcineurin
$[CaM_{total}]$	25	micromolar (μM)	the total concentration of calmodulin
d	0.9848	per second (s^{-1})	the nuclear import rate constant
D		squared micrometer per second ($\mu m^2 s^{-1}$)	Diffusion coefficient
E		millivolt (mV)	Nernst potential
$E_{Ca^{2+}}$		millivolt (mV)	Calcium Nernst potential
f	0.9624	per second (s^{-1})	the nuclear export rate constant
F	$96.49 \cdot 10^{12}$	pico-Coulomb per micromolar ($pC\mu M^{-1}$)	Faraday's constant
g		micro-Siemens (μS)	Membrane conductance
$\bar{g}$	$116 \cdot 10^{-3}$	micro-Siemens (μS)	Maximal conductance
h		$(-)$	Inactivation variable
$h_{Ca^{2+}}$		$(-)$	Calcium inactivation variable
i	1	$(-)$	Integral power of hypothetical activation variable
I		nano-Ampere (nA)	Ionic current
$I_{Ca^{2+}}$		nano-Ampere (nA)	Calcium current
j	1	$(-)$	Integral power of hypothetical inactivation variable
K	$10 \cdot 10^{-3}$	millimolar (mM)	Concentration at which the inactivation is halfway
K_1	4.3	micromolar (μM)	the binding constant of Pmc1
K_2	0.1	micromolar (μM)	the binding constant of Pmr1

Symbol	Value	Unit	Description
K_3	100	micromolar (μM)	the binding constant of Vcx1
k_c	10		the feedback control constant
k_{on}	$8.17 \cdot 10^{15}$	$M^{-n}s^{-1}$	the forward rate constant of Eq. 3.12
k_{off}	0.675	per second (s^{-1})	the backward rate constant of Eq. 3.12
k_M^+	8.3	$(\mu M)^{-3}s^{-1}$	the forward rate constant of Eq. 3.2
k_M^-	1.0798	per second (s^{-1})	the backward rate constant of Eq. 3.2
k_N^+	0.083	$(\mu M)^{-1}s^{-1}$	the forward rate constant of Eq. 3.4
k_N^-	1.0272	per second (s^{-1})	the backward rate constant of Eq. 3.4
K_x	500	micromolar (μM)	the binding constant of Transporter X
L_0	$10^{-N/2}$	$(-)$	the basic equilibrium constant
m		$(-)$	Activation variable
m_∞		$(-)$	Steady state value of m
N	13	$(-)$	the number of relevant regulatory phosphorylation sites
r		micrometer (μm)	Cell radius
t		millisecond (ms)	Time
V		millivolt (mV)	Voltage
V_1	500	micromolar per second ($\mu M/s$)	the rate parameter of Pmc1
V_2	1.67	micromolar per second ($\mu M/s$)	the rate parameter of Pmr1
V_3	167	micromolar per second ($\mu M/s$)	the rate parameter of Vcx1
V_n	$30 \cdot 10^{-15}$	liter (l)	Cell volume
V_x	16.7	micromolar per second ($\mu M/s$)	the rate parameter of Transporter X
α	0.9183	per second (s^{-1})	the growth constant rate
λ	5	$(-)$	the increment factor

Appendix B

Results basic calcium model

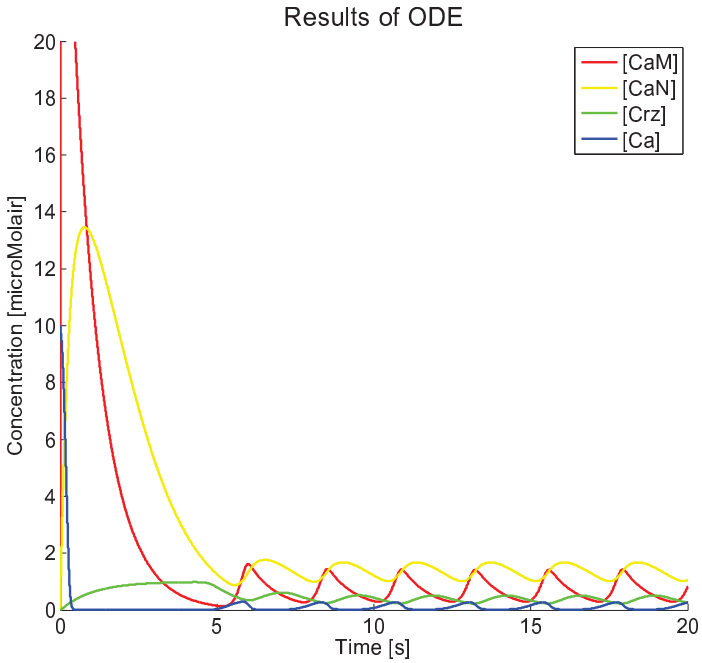

Figure B.1: Initial value $[Ca^{2+}] = 10\mu M$

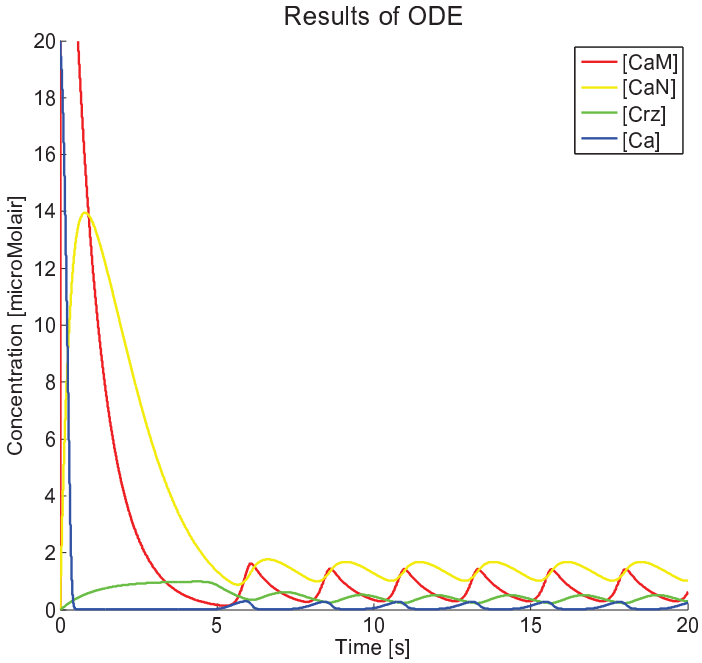

Figure B.2: Initial value $[Ca^{2+}] = 10\mu M$

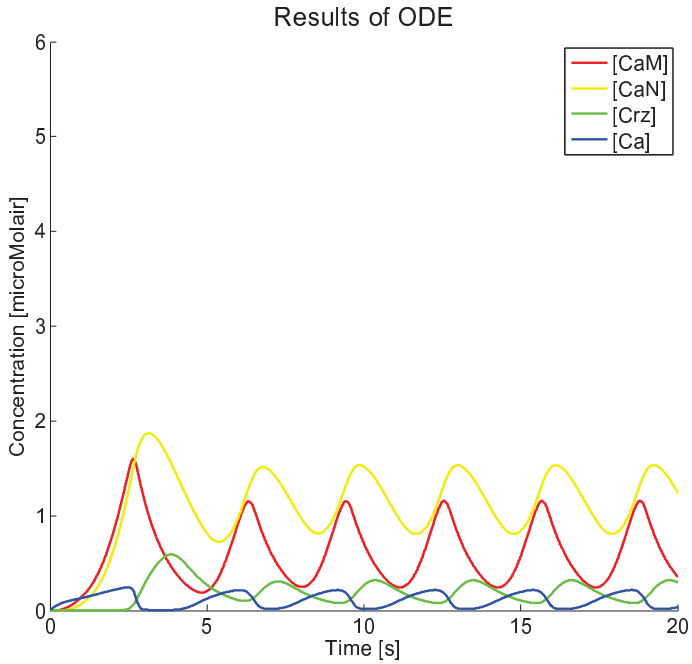

Figure B.3: Initial value $[Ca^{2+}] = 0\mu M$, $[Ca^{2+}]_{ex} = 10\mu M$

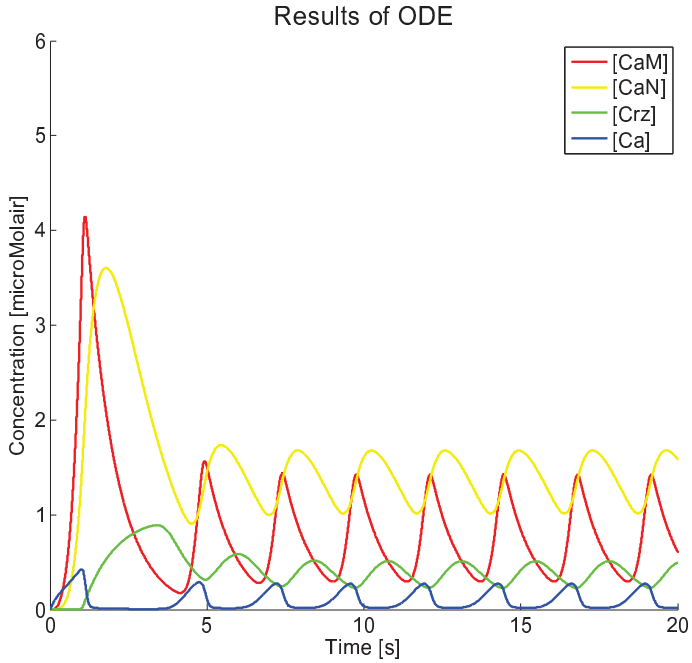

Figure B.4: Initial value $[Ca^{2+}] = 0\mu M$, $[Ca^{2+}]_{ex} = 25\mu M$

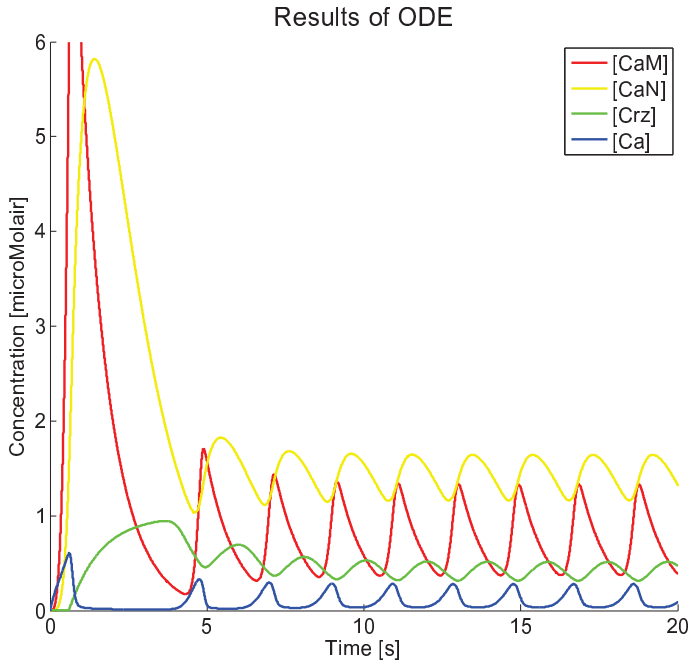

Figure B.5: Initial value $[Ca^{2+}] = 0\mu M$, $[Ca^{2+}]_{ex} = 50\mu M$

Appendix C

Results total calcium model

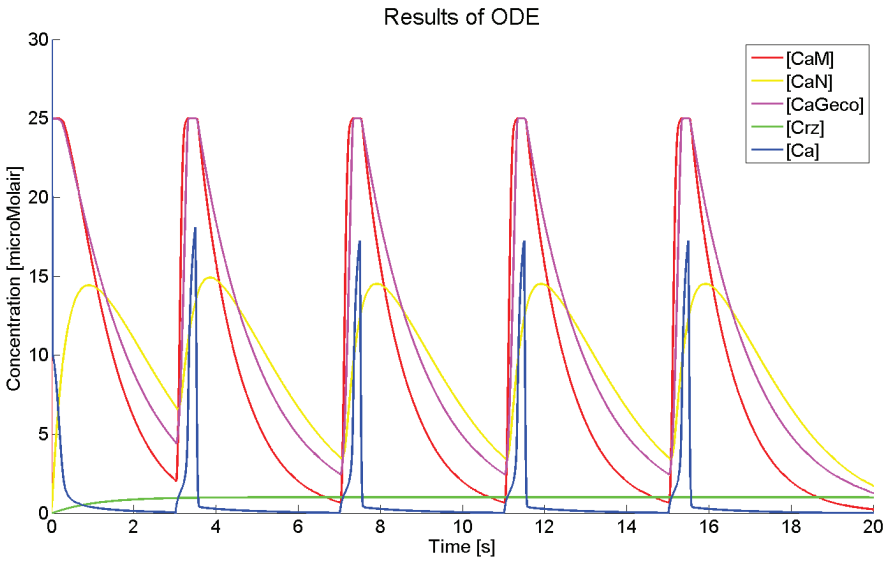

Figure C.1: Pulse duration: 0.5 seconds

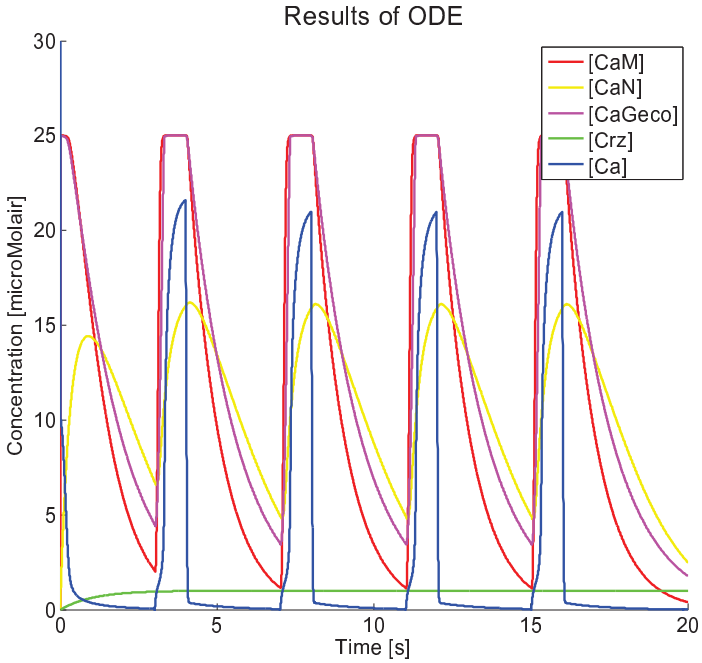

Figure C.2: Pulse duration: 1 second

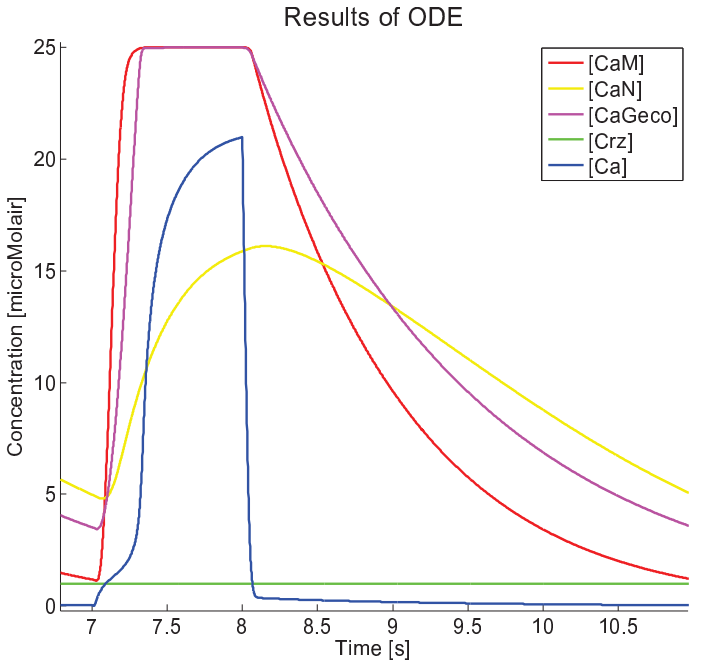

Figure C.3: Pulse duration: 1 second

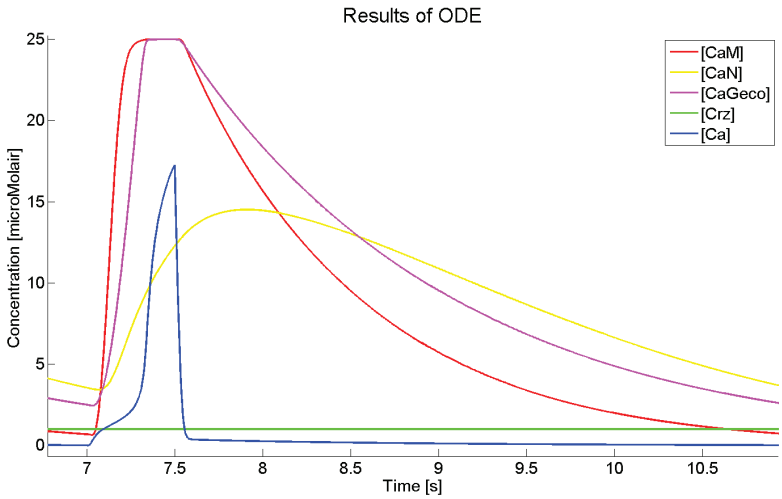

Figure C.4: Pulse duration: 0.5 seconds

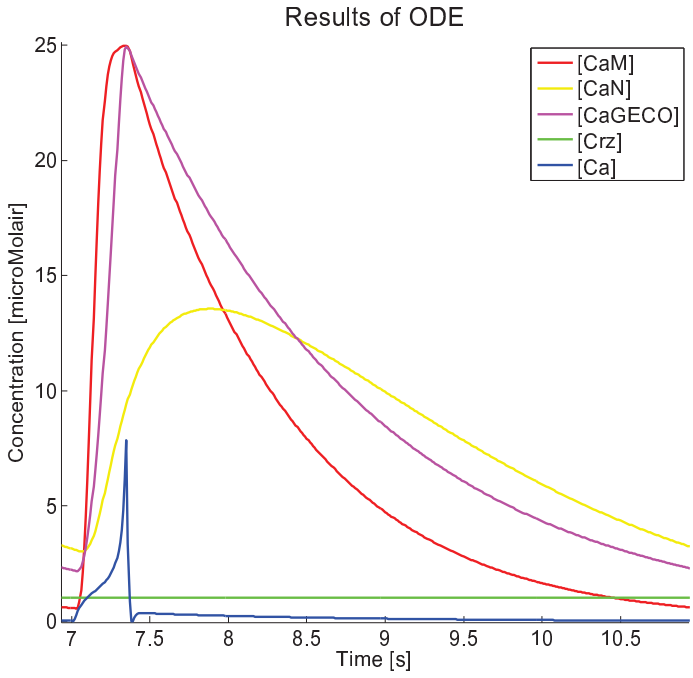

Figure C.5: Pulse duration: 0.35 seconds

Appendix D

Conformational switch model

The so called conformation switch model was firstly proposed by Okamura *et al* [17], based on their experimental study of NFAT1 phosphorylation states:

1. NFAT1 can assume two different structures, an active conformation and an inactive conformation.
2. The phosphorylation state of certain residues affects the global conformation of the portein. Therefore the probabilities of assuming the active and inactive conformations depend on the phosporylation state.
3. The active conformation is favored in the dephosporylated state, while the inactive conformation is favored in the phosphorylated state
4. The active conformation is imported into the nucleus, the inactive conformation is exported from the nucleus.

Later, Salazar *et al* further developed this concept into a fully mathematical form [18].

By describing the conformational switch model as a protein network and using the rapid equilibrium approximation [18], we can use the following equation to describe the kinetics of the total nuclear Crz1 fraction which is denoted by Crz(t) [12]:

$$\frac{dCrz(t)}{dt} = d \cdot \phi \cdot (1 - Crz(t)) - f \cdot \psi \cdot Crz(t) \tag{D.1}$$

where d denotes the import rate constant, f denotes the export rate constant, ϕ denotes the ratio of the fraction of the cytosolic active conformation over the total cytosolic fraction and ψ denotes the ratio of the fraction of nuclear inactive conformation over the total nuclear fraction. Concerning the number of cytosolic active, a_n, and inactive conformations, i_n, with n phosphorylated residues, ϕ can be calculated as follows [12]:

$$\begin{aligned}\phi &= \frac{\sum_{n=0}^{N} a_n}{\sum_{n=0}^{N}(a_n + i_n)} \\ &= \frac{1}{1 + \sum_{n=0}^{N} i_n / \sum_{n=0}^{N} a_n} \\ &= 1/(1 + L_0 \cdot \frac{(\lambda k/c)^{N+1} - 1}{\lambda k/c - 1} \cdot \frac{k/c - 1}{(k/c)^{N+1} - 1}) \end{aligned} \tag{D.2}$$

where k and c denote kinase and calcineurin activity in the cytosol respectively. Capital letters K and C are the corresponding activity in the nucleus. N is the number of relevant regulatory phosporylation sites, experimental data shows that $N = 13$ in the case of NFAT1. L_0 denotes the basic equilibrium constant and λ is the increment factor. The small case letters a_n and i_n $(n = 0, 1, 2...N)$ denote cytosolic active and inactive conformations with n phosphorylated residues respectively [12].

Under the assumption of $k/c = K/C$ we can calculate $\psi = 1 - \phi$. Therefore ϕ can be regarded as a function of k/c. If we assume that the kinase level is a constant and further express the concentration of activated calcineurin, CaN(t), in dimensionless units relative to this constant, then:

$$\phi(k/c) = \phi(1/(c/k)) = \phi(1/CaN(t)) \tag{D.3}$$

Now we can rewrite the kinetics equation **??** of the total nuclear fraction Crz1 as follows:

$$\frac{dCrz(t)}{dt} = d \cdot \phi(1/CaN(t)) \cdot (1 - Crz(t)) - f \cdot (1 - \phi(1/CaN(t))) \cdot Crz(t) \tag{D.4}$$

d denotes the import rate constant, f denotes the export rate constant and ϕ denotes the ratio of the fraction of the cytosolic active conformation over the total cytosolic fraction:

$$\phi(y) = 1/(1 + L_0 \cdot \frac{(\lambda y)^{N+1} - 1}{\lambda y - 1} \cdot \frac{y - 1}{(y)^{N+1} - 1}) \tag{D.5}$$

Appendix F

Model

Function file:

```
%MM_scriptm_ana

clear all;
close all;
set(gcf,'PaperUnits','centimeters');
set(gcf,'PaperSize',[12 9]);
set(gcf,'PaperPosition',[0 0 12 9]);
set(0,'defaultaxesfontsize',18);

print -painters -dpdf -r600 test.pdf
matrix_axis = [0 200 0 0.02];

Ca_ex = 1; %Extracellular calcium concentration (uM)

%Parameters of CaM
kmf = 8.3; %Forward rate constant (uM-3 s-1)
kmb = 100^(1/60); %Backward rate constant (s-1)
CaMtot = 25; %total calmodulin (bound + unbound)

%Parameters of CaN
knf = 8.3e-2; %Forward rate constant (uM-1 s-1)
knb = 5^(1/60); %Backward rate constant (s-1)
CaNtot = 25; %total calcineurin (bound + unbound), dimensionless

%Parameters of total nuclear fraction Crz1
khf = 0.4^(1/60); %nuclear import rate constant (s-1)
khb = 0.1^(1/60); %nuclear export rate constant (s-1)
nsites = 13; %number of relevant regulatory phosporylation sites
lzero = 10^(-nsites/2); %basic equilibrium constant
lamda = 5; %increment factor

%Parameters Michaelis Menten
kx = 500; %binding constant Transporter X (uM)
k1 = 4.3; %binding constant Pmc1 (uM)
k2 = 0.1; %binding constant Pmr1 (uM)
k3 = 100; %binding constant Vcx1 (uM)
```

```
vx = 16.7; %rate parameter of Transporter X (uM s-1)
v1 = 500; %rate parameter of Pmc1 (uM s-1)
v2 = 1.67; %rate parameter of Pmr1 (uM s-1)
v3 = 167; %rate parameter of Vcx1 (uM s-1)
kc = 10; %feedback control constant
alpha = 0.006^(1/60); %growth rate constant (s-1)

%Parameters of ionic current flow
i = 1; %Integral power of hypothetical activation variable
j = 1; %Integral power of hypothetical inactivation variable
g = 0.116; %Membrane conductance (microS (microSiemens))
K = 0.01e3; %Halfway inactivation concentration (uM)
Vn = 30e-15; %Volume of the cell (l)

%Parameters Geco kinetics
nhill = 2.6; %number of binding calcium
kgf = 8.17e15; %forward rate constant
kgb = 0.675; %backward rate constant
Gectot = 25; %total GECO (bound + unbound)

%Initial Conditions:
x0 = [10^-8 10^-8 10 10^-8 25 0.41];

%Parameter vector
par = [i, j, g, K, Vn, Ca_ex, kmf, kmb, CaMtot, knf, knb, CaNtot, khf, ...
    khb, nsites, lzero, lamda, kx, k1, k2, k3, vx, v1, v2, v3, kc, alpha, ...
    nhill, kgf, kgb, Gectot];
%Addressing the parameters

%Integrate ODEs:
tspan = [0:0.01:20]; %Time span (s)
odeoptions = odeset('RelTol',1e-4,'AbsTol',1e-6,'NonNegative', [1 1 1 1 ...
    1]); %Tolerances
[t,x] = ode15s(@MM_odem_ana_v6,tspan,x0,odeoptions,par);

%Plot results:
h=figure('position',[100 0 1100 ...
    1100],'paperpositionmode','auto','color','none','InvertHardcopy','off');
hold on;
title('Results of ODE','FontSize',22)
axis([0 20 0 50]);
xlabel('Time [s]')
ylabel('Concentration [microMolair]')
hl1 = line(t,x(:,1),'Color','r','LineWidth',2);
hl2 = line(t,x(:,2),'Color','y','LineWidth',2);
hl3 = line(t,x(:,3),'Color','m','LineWidth',2);
hl4 = line(t,x(:,4),'Color','g','LineWidth',2);
hl5 = line(t,x(:,5),'Color','b','LineWidth',2);
legend([hl1 hl2 hl3 hl4 hl5],{'[CaM]' '[CaN]' '[CaGECO]' '[Crz]' '[Ca]'});
hold off;
```

ODE-solver:

```
function [f] = MM_odem_ana_v6(t,x,par)

%State variables
CaM = x(1); %Concentration calcium-calmodulin combination (uM)
CaN = x(2); %Concentration calcium-calcineurin combination (uM)
CaGeco = x(3); %Concentration calcium-GECO combination (uM)
Crz = x(4); %Crz concentration (uM)
Ca = x(5); %Cystolic calcium concentration (uM)
m = x(6); %Hypothetical activation variable (mV)

%Voltage (mV)
if (t>3 && t<=4)
    V = 32;
else
    if (t>7 && t<=8)
        V=32;
    else
        if (t>11 && t <=12)
            V=32;
        else
            if (t>15 && t<=16)
                V=32;
            else
                V=-50;
            end
        end
    end
end

%Parameters of ionic current flow
i = par(1); %Integral power of hypothetical activation variable
j = par(2); %Integral power of hypothetical inactivation variable
g = par(3); %Membrane conductance (s)
K = par(4); %Halfway inactivation concentration (uM)
Vn = par(5); %Volume of the cell (L)
Ca_ex = par(6); %Extracellular calcium concentration (uM)
F = 9.649e10; %Faraday's constant (Coulomb uM^{-1})

m_inf = 1/(1 + exp(-(V-3)/8)); %Steady state value of hypothetical ...
    activation variable (mV)
tau_m = 7.8/(exp((V-3)/8) + exp(-(V-3)/8)); %Time constant (mV^{-1})
%%% h = K/(K+Ca); %Hypothetical inactivation variable (uM)
%%% E = 12.5*log(Ca_ex/Ca); %Reversal potential (mV)

%Parameters of CaM
kmf = par(7); %Forward rate constant (uM-3 s-1)
kmb = par(8); %Backward rate constant (s-1)
CaMtot = par(9); %total calmodulin (bound + unbound)

%Parameters of CaN
knf = par(10); %Forward rate constant (uM-1 s-1)
knb = par(11); %Backward rate constant (s-1)
CaNtot = par(12); %total calcineurin (bound + unbound)

```

```
%Parameters of total nuclear fraction Crz1
khf = par(13); %import rate constant (s-1)
khb = par(14); %export rate constant (s-1)
nsites = par(15); %number of relevant regulatory phosporylation sites
lzero = par(16); %basic equilibrium constant
lamda = par(17); %increment factor

%Parameters Michaelis Menten
kx = par(18); %binding constant of Transporter X (uM)
k1 = par(19); %binding constant of Pmc1 (uM)
k2 = par(20); %binding constant of Pmr1 (uM)
k3 = par(21); %binding constant of Vcx1 (uM)
vx = par(22); %rate parameter of Transporter X (uM s-1)
v1 = par(23); %rate parameter of Pmc1 (uM s-1)
v2 = par(24); %rate parameter of Pmr1 (uM s-1)
v3 = par(25); %rate parameter of Vcx1 (uM s-1)
kc = par(26); %feedback control constant
alpha = par(27); %growth rate constant (s-1)

%Parameters Geco kinetics
nhill = par(28); %number of binding calcium
kgf = par(29); %forward rate constant
kgb = par(30); %backward rate constant
Gectot = par(31); %total GECO (bound + unbound)

%ODEs
f(1) = (kmf*(CaMtot-CaM)*Ca^3) - (kmb*CaM);
f(2) = (knf*(CaNtot-CaN)*CaM) - (knb*CaN);
f(3) = (kgf*(Gectot-CaGeco)*((Ca*10^-6)^nhill)) - (kgb*CaGeco);
f(4) = khf*(1/(1 + ((lzero * ((lamda/CaN)^(nsites+1)-1)/((lamda/CaN)-1)...
    * ((CaN^-1 - 1)/(CaN^(-(nsites+1))-1))))))*(1-Crz)...
    - (khb*(1-((1/(1 + ((lzero * ((lamda/CaN)^(nsites+1)-1)/((lamda/CaN)-1)...
    * ((CaN^-1 - 1)/(CaN^(-(nsites+1))-1)))))))*Crz);
f(5) = ((vx*Ca_ex)/(kx+Ca_ex))... %transporter X
    - (Crz * (1/(1 + (lzero *(((lamda/CaN)^(nsites+1)-1)/((lamda/CaN)-1))...
    * (((CaN^-1) - 1)/(CaN^(-(nsites+1))-1))))) * ...
    ((v1*Ca)/(k1+Ca)))...          %Pmc1
    - (Crz * (1/(1 + (lzero *(((lamda/CaN)^(nsites+1)-1)/((lamda/CaN)-1))...
    * (((CaN^-1) - 1)/(CaN^(-(nsites+1))-1))))) * ...
    ((v2*Ca)/(k2+Ca)))...          %Pmr1
    - ((1.0 / (1.0+kc*CaN)) * ((v3*Ca)/(k3+Ca)))... %Vcx1
    - (alpha * Ca)...
    - (-g*m^(i)*(K/(K+Ca))^(j)*(V - (12.5*log(Ca_ex/Ca))))/(2*F*Vn)...
    + nhill * ((kgb * CaGeco) - (kgf * (Ca*10^-6)^nhill * (Gectot - CaGeco)));
f(6) = ((m_inf - m)/(tau_m)); %m

f = f(:);
```

Bibliography

[1] M. Schmidt, A. Kelle, A. Ganguli-Mitra and H. de Vriend, *Synthetic Biology: The Technoscience and its Societal Consequences*, (2010)

[2] S. Benner and M. Sismour, *Synthetic Biology*, Nature Reviews, Vol. 6, (2005)

[3] M. Elowitz and S. Leibler, *A Synthetic Oscillatory Network of Transcriptional Regulators*, Nature Reviews, Vol. 403, (2000)

[4] T. Gardner, C. Cantor and J. Collins, *Construction of a Genetic Toggle Switch in Escherichia Coli*, (2000)

[5] I. Chen and D. Dubnau, *DNA Uptake During Bacterial Transformation*, Nature Reviews, Vol. 2, (2004)

[6] L. Cobo and I. Akyildiz, *Bacteria-Based Communication in Nanonetworks*, Nano Communication Networks, (2010)

[7] B. Alberts, A. Johnson, J. Lewis, J. Wilson and T. Hunt, *Molecular Biology of the Cell*, (2008)

[8] J. Berg, J. Tymoczko and L. Stryer, *Biochemistry*, (2012)

[9] K. Iida, T. Taba and H. Iida, *Molecular Cloning in Yeast by In Vivo Homologous Recombination of the Yeast Putative $\alpha 1$ Subunit of the Voltage-Gated Calcium Channel*, FEBS Letters 576, (2004)

[10] Y. Zhao, S. Araki, J. Wu, T. Teramoto, Y. Chang, M. Nakano, A. Abdelfattah, M. Fujiwara, T. Ishihara, T. Nagai and R. Campbell, *An Expanded Palette of Genetically Encoded Ca^{2+} Indicators*, Science, Vol. 333, (2011)

[11] A. Miseta, L. Fu, R. Kellermayer, J. Buckley, D.M. Bedwell, *The Golgi Apparatus plays a significant role in the maintainance of Ca^{2+} homeostasis in the vps33 vacuolar biogenesis mutant of Saccharomyces cerevisiae*, J. Biol. Chem. 274: 5939-5947, (1999).

[12] J. Cui, *Mathematical modeling of metal ion homeostasis and signaling systems*, (2009).

[13] C. Balemans *Modeling of the calcium dynamics in neuronal cells for the International Genetically Engineered Machine competition*, (2012).

[14] H. Kitano, *Systems biology : a brief overview*, Nature 295: 1662-1664, (2002).

[15] M.S. Cyert, *Genetic analysis of calmodulin and its targets in Sacchromyces cerevisiae*, Annu. Rev. Genet. 35: 647-672, (2001).

[16] A. Stathopoulos-Gerontides, J.J. Guo, M.S. Cyert, *Yeast calcineurin regulates nuclear localization of the Crz1 transcription factor through dephosphorylation*, Genes and Dev. 13: 798-803, (1999)

[17] H. Okamura, J. Aramburu, C. Garca-Rodrguez, et al. *Concerted dephosphorylation of the transcription factor NFAT1 induces a conformational switch that regulates transcriptional activity*, Mol. Cell 6: 539-550, (2000).

[18] C. Salazar and T. Hfer, *Allosteric regulation of the transcription factor NFAT1 by multiple phosphorylation sites: a mathematical analysis*, J. Mol. Biol. 327: 3145, (2003).

[19] C. Koch and I. Segev (editors), *Methods in Neuronal Modeling: From Synapses to Networks*, (1989)

[20] J. Malmivuo, R. Plonsey, *Bioelectromagnetism*, (1995)

[21] M. Kumar, S. Ahmad, E. Ahmad, M. Saifi and R. Khan, *In Silico Prediction and Analysis of Caenorhabditis EF-hand Containing Proteins*, Pubmed, (2012)

[22] D. Sterratt, B. Graham, A. Gillies and D. Willshaw, *Principles of Computational Modelling in Neuroscience*, (2011)

[23] M. Breit, *Masterthesis: Sensitivity Analysis of Biological Pathways*, (2004)